Power and Speed Control of Brushless Doubly-Fed Induction Generators

Hamidreza Mosaddegh-Hesar
Department of Electrical and Computer Engineering
University of Saskatchewan
Saskatoon, SK, Canada
pvt356@mail.usask.ca

Xiaodong Liang
Department of Electrical and Computer Engineering
University of Saskatchewan
Saskatoon, SK, Canada
xil659@mail.usask.ca

Salman Abdi
School of Engineering
University of East Anglia
Norwich, UK
s.abdi-jalebi@uea.ac.uk

***Abstract*—The brushless doubly fed induction generator (BDFIG) with a partially rated converter has characteristics of both a squirrel cage induction generator and a conventional synchronous generator. Its control is very challenging due to the machine's complicated structure, which requires an effective controller to stabilize it within its normal speed range and under various steady state and dynamic operations. In this paper, a comprehensive nonlinear vector control scheme is proposed for BDFIGs, where the speed control is achieved through the model reference adaptive control (MRAC), while the reactive power and electromagnetic torque control are achieved through a hybrid controller by combining the sliding mode and proportional-integrator (PI) control. Simulations using MATLAB/Simulink indicate that the proposed nonlinear control structure yields superior dynamic response when subjected to input mechanical power and reference speed changes when compared to a linear PI controller.**

Keywords—Brushless doubly fed induction generator, model reference adaptive system, proportional-integrator (PI) controller, reactive power control, sliding mode controller, speed control.

I. INTRODUCTION

The brushless doubly-fed induction generator (BDFIG) has a single frame with two balanced three-phase stator windings, known as the "power winding (PW)", which is directly connected to the grid and responsible for a substantial portion of power exchange between the grid and the machine, and the "control winding (CW)", which is connected to the grid through a back-to-back partial rated converter [1]. In recent years, there has been increased interest in the BDFIG's research and development due to its advantages, such as eliminating brushes and employing a converter with a capacity of approximately 30% of the generator's total capacity [2], [3]. However, the BDFIG lacks inherent stability over its operating speed range, and requires an effective controller to stabilize it under various steady state and dynamic operations [4].

To achieve the optimal performance under steady state and dynamic operating conditions for BDFIGs, closed-loop control methods can be used. In [5], a predictive sliding mode controller is presented for simple and effective BDFIG power control in the generation mode. To track desired values of active and reactive power, the proposed controller considers the current components in the stationary frame as sliding surfaces. To select the appropriate voltage vector to feed the CW, a cost function is defined based on quadratic errors of the currents, and the particle swarm optimization (PSO) algorithm is used to determine optimal values of the controller's gains. In [6], the performance of the BDFIG-based wind turbine is investigated under sudden disturbances due to load variations at the wind turbine terminals and wind speed variations, where a simple control scheme based on the proportional-integral (PI) controller is used to maintain its voltage constant at the nominal value during sudden load and wind speed changes. In [7], a voltage control strategy based on the resonant sliding mode control method for wind turbine applications is presented, where control inputs are determined by the speed error and the PW voltage. Ref. [8] presents a vector control method for BDFIGs, and the proposed vector control is implemented on the PW flux frame with the ability to simultaneously control the speed and reactive power using a PI controller. In [9], to investigate the possibility of implementing the speed vector control on BDFIGs, two inner loops are designed to control the PW and CW currents and minimize the coupling between the two stator windings, and an external loop is designed to control the speed; for the inner loops, dynamic equations of the machine are used to determine the flow controllers.

To control a BDFIG without speed sensors, a model reference adaptive observer is designed based on the current error of the CW in [10] by proving the stability of the observer and analyzing its steady state and dynamic performance. In [11], an approach based on a second-order sliding mode controller is proposed for direct control of active and reactive power of a BDFIG, providing quick responses to transient conditions and robustness to uncertainties caused by changing parameters. In [12], a vector control based on the proportional-integral-resonant controller (PIRC) is proposed for BDFIGs in wind turbine applications, and the machine's dynamic characteristics are studied under unbalanced conditions for the control objectives: to eliminate active and reactive power ripples, and achieve three-phase balanced currents for PW and CW.

Due to the relatively complex structure of a BDFIG, its control is very challenging, and non-linear control methods are necessary to control its speed, electromagnetic torque and

reactive power. In this paper, a new control system for BDFIGs is proposed based on two nonlinear control methods, the model reference adaptive control (MRAC) and the sliding mode control. In this control system, the generator's speed control is realized by the MRAC method; while the generator's reactive power and electromagnetic torque control is realized by a hybrid controller, a combination of the sliding mode control and PI control. The proposed control system guarantees steady state and dynamic performance of BDFIGs, which is validated by simulating various operating scenarios by MATLAB/Simulink.

II. The Model of BDFIGs

The dynamic model of a BDFIG in the PW flux frame is expressed as follows [1]:

$$\vec{V}_p = R_p\vec{I}_p + \frac{d\vec{\lambda}_p}{dt} + j\omega_p\vec{\lambda}_p \tag{1}$$

$$\vec{\lambda}_p = L_p\vec{I}_p + L_{pr}\vec{I}_r \tag{2}$$

$$\vec{V}_c = R_c\vec{I}_c + \frac{d\vec{\lambda}_c}{dt} + j(\omega_p - (p_p + p_c)\omega_r)\vec{\lambda}_c \tag{3}$$

$$\vec{\lambda}_c = L_c\vec{I}_c + L_{cr}\vec{I}_r \tag{4}$$

$$\vec{V}_r = 0 = R_r\vec{I}_r + \frac{d\vec{\lambda}_r}{dt} + j(\omega_p - p_p\omega_r)\vec{\lambda}_r \tag{5}$$

$$\vec{\lambda}_r = L_r\vec{I}_r + L_{pr}\vec{I}_p + L_{cr}\vec{I}_c \tag{6}$$

The electromagnetic torque T_e and reactive power Q_p of the PW are obtained by [13]:

$$T_e = \frac{3}{2}p_p\left|\vec{\lambda}_p\right|i_{pq} + \frac{3}{2}p_c\left[-\frac{L_{cr}}{L_{pr}}\left|\vec{\lambda}_p\right|i_{cq} + \frac{L_pL_{cr}}{L_{pr}}(i_{pd}i_{cq} - i_{pq}i_{cd})\right] \tag{7}$$

$$Q_p = \frac{3}{2}(v_{pq}i_{pd} - v_{pd}i_{pq}) \tag{8}$$

where the subscripts *p*, *c*, and *r* in (1)-(6) represent the PW, CW, and rotor, respectively. Parameters and variables used in (1)-(6) are shown in Table I.

TABLE I. Parameters and Variables

Symbol	Parameter
$\vec{V}$, $\vec{I}$, $\vec{\lambda}$	Vectors of the voltage, current and flux
R_p R_c, R_r	Resistances of PW, CW and the rotor
L_p, L_c, L_r	Self-inductances of PW, CW and the rotor
L_{pr}, L_{cr}	Mutual inductances between the stators (PW and CW) and the rotor
ω	Angular speed
p	Pole pair number

III. Speed Control Based on The Model Reference Adaptive Control

The Massachusetts Institute of Technology (MIT) rule [14] does not provide a guarantee of the closed-loop stability for an adaptive controller. Therefore, in this paper, the Lyapunov theory is utilized to adapt the MRAC design for the speed control of the BDFIG. Initially, a differential equation with adjustable parameters is formulated to describe the error. Subsequently, a Lyapunov function and a tuning mechanism are established to reduce the error towards zero. Given that the time constant of electrical circuits is significantly smaller than that of the mechanical system, a BDFIG can be modeled via the first-order differential equation for the closed-loop speed control through the reference model, as illustrated in Fig. 1:

$$\dot{\omega}_r = -a\omega_r + b\Delta\omega_r^* \tag{9}$$

where *a* and *b* are coefficients of the system. The superscript * indicates the speed reference value. To achieve the desired response, the reference model is selected as follows:

$$\dot{\omega}_{rm} = -a_m\omega_{rm} + b_m\omega_r^* \tag{10}$$

where a_m and b_m are coefficients of the reference model. By adjusting a_m and b_m, the optimal system performance can be achieved, and the system output will follow the reference model output. According to Fig. 1, the error is defined as follows:

$$e = \omega_r - \omega_{rm} \tag{11}$$

The controller is expressed by

$$\Delta\omega_r^* = \theta_1\omega_r^* - \theta_2\omega_r \tag{12}$$

By differentiating (11) with respect to time, and substituting (9) and (10) into (12), we have

$$\dot{e} = \dot{\omega}_r - \dot{\omega}_{rm} = -a_m e - (b\theta_2 + a - a_m)\omega_r + (b\theta_1 - b_m)\omega_r^* \tag{13}$$

To achieve an adjustment mechanism that brings the parameters θ_1 and θ_2 to the desired values, a Lyapunov function is defined as follows:

$$V(e,\theta_1,\theta_2) = \frac{1}{2}\left(e^2 + \frac{1}{b\gamma}(b\theta_1 - b_m)^2 + \frac{1}{b\gamma}(b\theta_2 + a - a_m)^2\right) \tag{14}$$

In (14), it is assumed that $b\gamma > 0$, so the Lyapunov function would be positive definite. To guarantee the MRAC's stability, the following conditions must be met:

$$\begin{cases}\dot{V} < 0 & \forall e \neq 0\\ \dot{V} = 0 & \forall e = 0\end{cases} \tag{15}$$

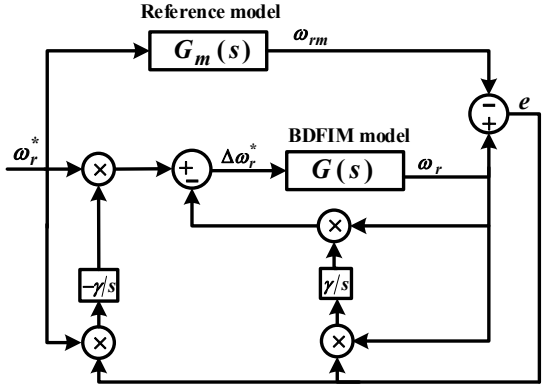

Fig. 1. The MRAC's block diagram for the speed control of a BDFIG.

Consequently, based on (13) and (14), we have:

$$\dot{V} = e\dot{e} + \frac{1}{\gamma}(b\theta_1 - b_m)\dot{\theta}_1 + \frac{1}{\gamma}(b\theta_2 + a - a_m)\dot{\theta}_2$$
$$= -a_m e^2 + \frac{1}{\gamma}(b\theta_1 - b_m)(\dot{\theta}_1 + \gamma\omega_r^* e) \quad (16)$$
$$+ \frac{1}{\gamma}(b\theta_2 + a - a_m)(\dot{\theta}_2 - \gamma\omega_r e)$$

As a result, to satisfy (15), the adaptive rules are determined based on

$$\dot{\theta}_1 = -\gamma\omega_r^* e, \quad \dot{\theta}_2 = -\gamma\omega_r^* e \quad (17)$$

According to (16) and (17), to prove the asymptotic stability of the closed loop system, the Barbalat's lemma [15] is used in this paper. Therefore, the second order derivative of (16) by taking into account the adaptive rules is

$$\ddot{V} = -2a_m e\dot{e} \quad (18)$$

Based on (14) and (16), e is bounded. The reference signal ω_{rm} and its first order derivative and the signal ω^*_{rm} are also bounded. Based on (11), ω_r is bounded. Based on (13), the error derivative is bounded, so Eq. (18) is bounded, and based on the Barbalat's lemma, the asymptotic stability can be guaranteed.

IV. The Hybrid Controller with Sliding Mode and PI Control

Considering the non-linear nature of electric machines, if the reference voltage is produced by non-linear controllers, the electric drive can perform better [16]. The sliding mode controller of electric drives has advantages due to its robustness to changes and uncertainties in the system parameters under control, fast dynamic response, and the ability to compensate for effects of disturbances and uncertainties. However, its robustness is only related to its sliding phase, and the reaching phase is designed in such a way that the paths of the mechanical state of the system lead to the sliding phase as quickly as possible. Therefore, conventional sliding mode controllers have this basic weakness that they may not be able to maintain their stability in the reaching phase with respect to uncertainties and disturbances [17]; these controllers also cause a chattering phenomenon.

To improve the system consistency with respect to uncertainties and eliminate the chattering of the control system, a new hybrid controller, a combination of the sliding mode control and PI control, is proposed in this paper. This hybrid controller is simple to implement; has desirable characteristics of a linear controller, such as with smooth and chattering free operations; maintains the merit of a robust sliding mode controller when dealing with uncertainties; and does not depend on the system's parameters. Its control parameters are reactive power and the electromagnetic torque of the generator. The sliding surface is defined by

$$S_{Q_p} = e_{Q_p} + c_{Q_p} \cdot \int e_{Q_p} \quad (19)$$

$$S_{T_e} = e_{T_e} + c_{T_e} \cdot \int e_{T_e} \quad (20)$$

where the errors of reactive power and the torque are equal to

$$e_Q = Q_p^* - Q_p \quad (21)$$

$$e_{T_e} = T_e^* - T_e \quad (22)$$

The design constants c_{Qp} and c_{Te} lead to the desired dynamics in the sliding surface. The reference voltage is obtained at the output of the controller. The direct-axis (d-axis) component is produced by the reactive power control law, and the quadrature-axis (q-axis) component is produced by the torque control law as follows:

$$v_{cd}^* = (K_{PQ_p} + \frac{K_{IQ_p}}{s}).(e_{Q_p} + K_{VSCQ_p}.Sgn(S_{Q_p})) \quad (23)$$

$$v_{cq}^* = (K_{PTe} + \frac{K_{ITe}}{s}).(e_{Te} + K_{VSCTe}.Sgn(S_{Te})) \quad (24)$$

The parameters of the sliding mode controller are provided in Table II. By choosing appropriate coefficients for the sliding mode and PI control, the system response is robust and chattering free. In the transient state, the first term of (23) and (24) is much larger than the second term, and thus, the linear PI controller is dominant, i.e., during this period, the control system is essentially a PI controller. In the steady state, the second term including the sign function is dominant, and is passed through the PI controller to reduce the chattering phenomenon. The general block diagram of the proposed control system is shown in Fig. 2.

V. Simulation Results

In this section, to validate the proposed control method for BDFIGs, the simulation is conducted by MATLAB/Simulink using specifications of a BDFIG in Table III.

A. Speed Control

Since the rotor speed control is essential in various applications, Fig. 3 shows a comparison of speed responses using the proposed control method - MRAC and a conventional PI controller when the reference speed is changed from 0.6 $p.u.$ to 1.2 $p.u.$ at $t = 5\ sec$. The base speed of this generator is 500 rpm. According to Fig. 4, by changing the reference speed from 0.6 $p.u.$ to 1.2 $p.u.$, the generator speed changes from sub-synchronous speed to super-synchronous speed. The phase sequence of the CW current changes when the generator speed reaches 1 $p.u.$ (the natural speed).

TABLE II. Parameters of the Sliding Mode Contorller

Symbol	Parameter
s	Laplace operator
K_{PQ_p} , K_{ITe} , K_{PTe} , K_{IQ_p}	PI controller gains
K_{VSCQ_p} , K_{VSCTe}	Sliding mode controller gains

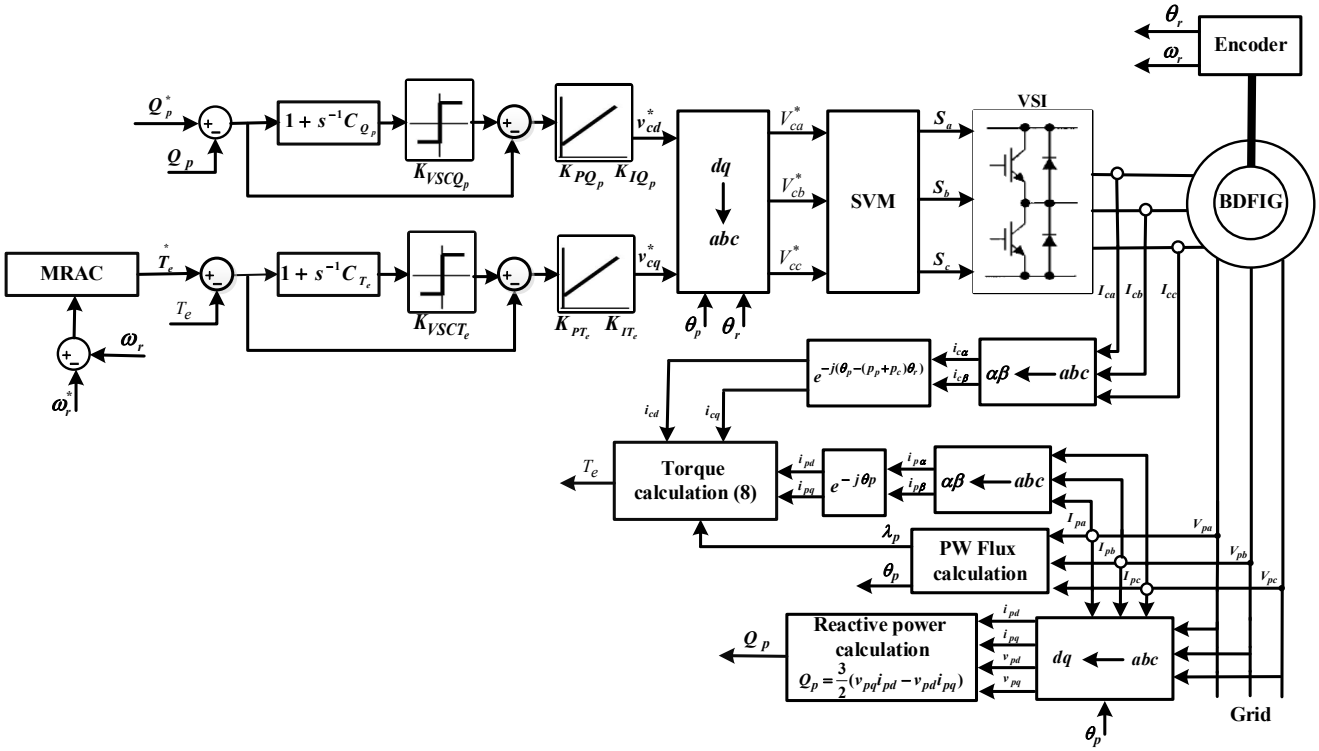

Fig. 2. The block diagram of the control system.

TABLE III. THE PARAMETERS OF THE BDFIG

Parameter	Value	Parameter	Value
PW/CW pole-pair	2/4	R_r (Ω)	1.1237
PW/CW rated voltage (V)	180	L_{pr} (H)	0.1863
PW/CW rated current (A)	10/4.5	L_{cr} (H)	0.0998
Natural speed (rpm)	500	L_{lp} (H)	0.0047
R_p (Ω)	1.3012	L_{lc} (H)	0.0053
R_c (Ω)	3.7171	L_{lr} (H)	0.0206

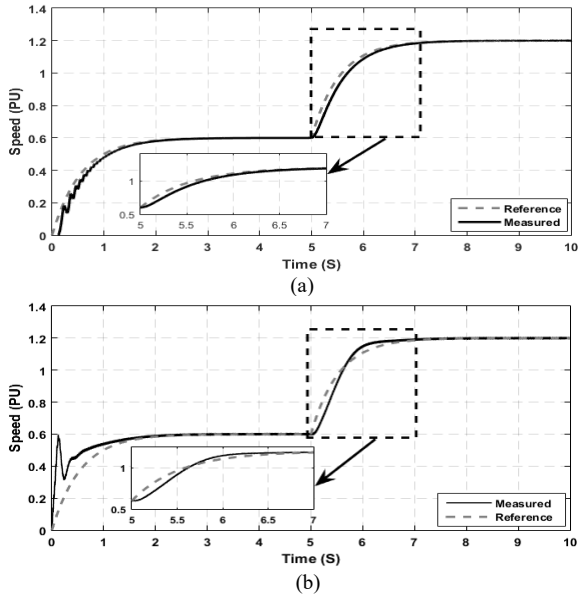

Fig. 3. Speed response of the BDFIG for a speed reference change: (a) the proposed control method - MRAC, (b) PI controller.

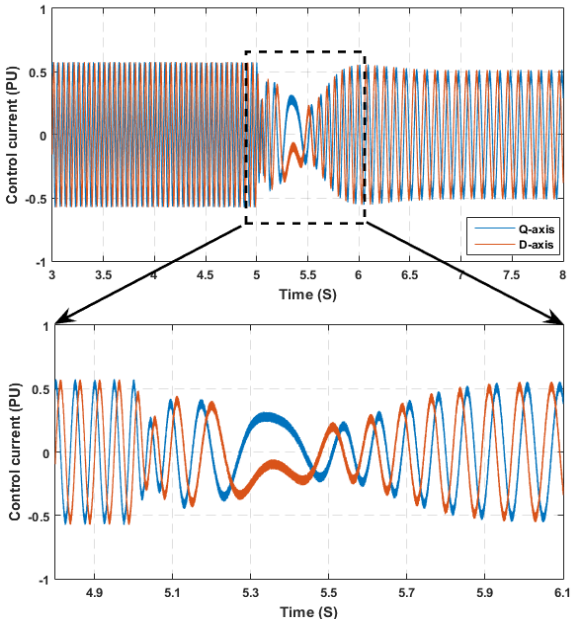

Fig. 4. The d-and q-axis components of the CW current of the BDFIG for a reference speed change.

Fig. 5 shows the speed responses when the input mechanical power is increased stepwise at $t = 5\,sec$, showing a faster response of the proposed MRAC speed controller than a PI controller. At the moment of the input power increase, the generator speed fluctuates around the reference value within a limited time, and the speed control is then executed well at a new input power.

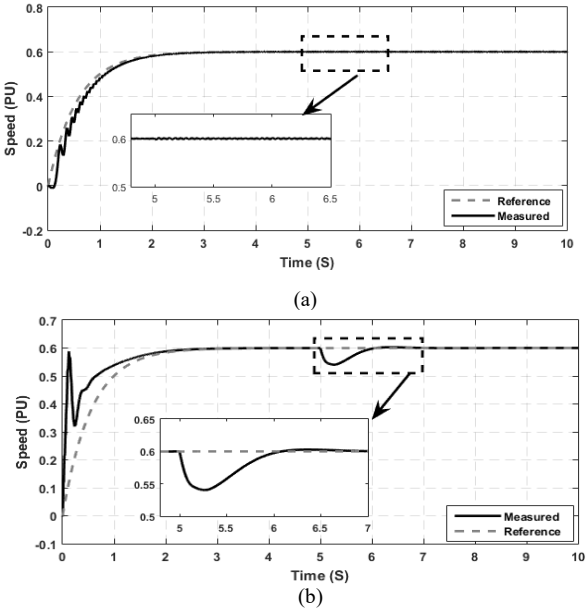

Fig. 5. Speed response of the BDFIG for an input mechanical power change: (a) the proposed control method - MRAC, (b) the PI controller.

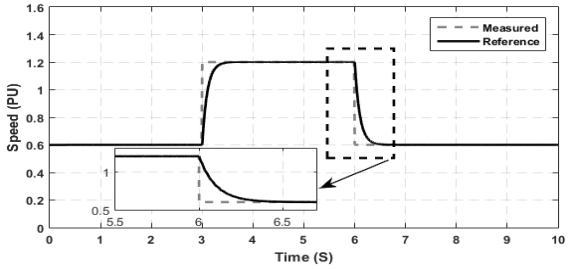

Fig. 6. The speed response of the BDFIG when the speed reference and input mechanical power are changed simultaneously.

Fig. 6 shows the response of the model reference controller to simultaneous changes of the reference speed and the input mechanical power. In this scenario, the reference speed increases from 0.6 $p.u.$ to 1.2 $p.u.$ at $t = 3\,sec$, and then decreases to the initial value of 0.6 $p.u.$ at $t = 6\,sec$. Simultaneously, as the speed reference changes, the input mechanical power increases from 0.25 $p.u.$ to 0.5 $p.u.$ at $t = 3\,sec$, and then decreases to the initial value of 0.25 $p.u.$ at $t = 3\,sec$. The proposed MRAC controller provides a desired dynamic speed response against the simultaneous step changes of both reference speed and input mechanical power of the BDFIG.

B. Reactive Power and Torque/Active Power Control

Fig. 7 shows the reactive power response of the generator with the hybrid controller and a conventional PI controller when the input mechanical power changes from 0.25 pu to 0.5 $p.u.$ at $t = 5\,sec$. At the moment of an input mechanical power change, the PW's reactive power overshoot with the hybrid controller is around 0.54 $p.u.$, but quickly reaches the reference value.

Figs. 8 and 9 show the active power response of the PW and the trajectory of the two-axes CW flux of the BDFIG for the same input mechanical power change as in Fig. 5, respectively.

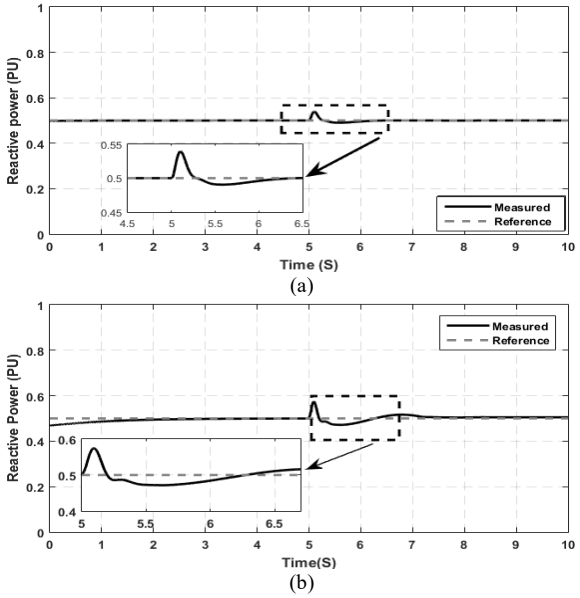

Fig. 7. Reactive power response of the BDFIG when subjected to an input mechanical power change: (a) Hybrid controller, (b) PI controller.

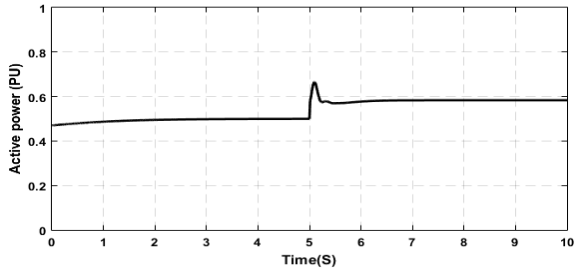

Fig. 8. Active power response of the BDFIG when subjected to an input mechanical power change.

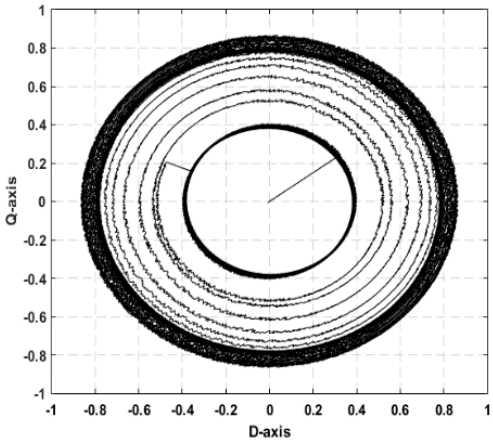

Fig. 9. The CW's two-axis flux trajectory of the BDFIG when subjected to an input mechanical power change.

VI. CONCLUSION

This paper introduces a nonlinear vector control approach for BDFIGs. The proposed method comprises two components: 1) speed control through model reference adaptive control, and 2) control of reactive power and electromagnetic torque/active power through a hybrid controller that integrates sliding mode and PI control. Ensuring stability and achieving the desired dynamic response during abrupt changes in input mechanical

power are crucial from the perspective of the machine operator. Simulation results for a BDFIG demonstrate the effectiveness of the proposed control method in maintaining stability and controlling the generator's speed, active power, and reactive power when facing variations in input mechanical power and speed references.

REFERENCES

[1] H. Mosaddegh-Hesar, H. Abootorabi Zarchi and G. A. Markadeh, "Modeling and Dynamic Performance Analysis of Brushless Doubly Fed Induction Machine Considering Iron Loss," *IEEE Transactions on Energy Conversion*, vol. 35, no. 1, pp. 193-202, March 2020.

[2] E. Abdi, A. Oraee, S. Abdi, and R. A. McMahon "Design of the Brushless DFIG for Optimal Inverter Rating", *7th IET International Conference on Power Electronics, Machines and Drives (PEMD)*, 2014.

[3] A. Oraee, E. Abdi, S. Abdi, and R. A. McMahon "A study of converter rating for brushless DFIG wind turbines", *2nd IET Renewable Power Generation Conference (RPG 2013)*, 2013.

[4] H. R. Mosaddegh-Hesar and H. Abootorabi Zarchi, "Variable Structure Direct Torque Control of Brushless Doubly Fed Induction Generator for Wind Turbine Applications," *22nd Iranian Conference on Electrical Engineering (ICEE)*, Tehran, Iran, 2014, pp. 671-676.

[5] A. Dountio, E.D. Kenmoe Fankem, G. Golam, "Control of a BDFIG Based on Current and Sliding Mode Predictive Approaches", *Journal of Control, Automation and Electrical Systems*, vol. 31, no. 1, pp. 636-647, Jan. 2020.

[6] K.S.A. EL-Naeem, G. El-Saady, A. Yousef, E.A. Ibrahim, "Anti-Colony PI Controllers Based High Performance Brushless Doubly Fed Induction Generator Driven by Wind Turbine", *Proceeding of the IEEE/ CPERE*, pp. 51-56, Aswan, Egypt, Feb. 2020

[7] K. Ji, S. Huang, "Direct Flux Control For Stand-Alone Operation Brushless Doubly Fed Induction Generators Using A Resonant-Based Sliding-Mode Control Approach", *Energies*, vol. 11, no. 4, pp. 220-228, April 2018.

[8] J. Poza, E. Oyarbide, I. Sarasola, M. Rodriguez, "Vector Control Design and Experimental Evaluation for the Brushless Doubly Fed Machine", *IET Electric Power Applications*, vol. 3, no. 4, pp. 247-256, July 2009.

[9] J. Yang, W. Tang, G. Zhang, Y. Sun, S. Ademi, F. Blaabjerg, Q. Zhu, "Sensorless control of brushless doubly fed induction machine using a control winding current MRAS observer", *IEEE Tran. on Industrial Electronics*, vol. 66, no. 1, pp. 728-738, Jan. 2019.

[10] R. Sadeghi, S.M. Madani, M. Ataei, M.R. Agha-Kashkooli, S. Ademi, "Super-twisting sliding mode direct power control of a brushless doubly fed induction generator", *IEEE Trans. on Industrial Electronics*, vol. 65, no. 11, pp. 9147-9156, Nov. 2018

[11] L. Sun, Y. Chen, J. Su, D. Zhang, L. Peng, Y. Kang, "Decoupling Network Design For Inner Current Loops Of Stand-Alone Brushless Doubly Fed Induction Generation Power System", *IEEE Trans. on Power Electronics*, vol. 33, no. 2, pp. 957-963, Feb. 2018.

[12] R. Tafazzoli-Mehrjardi, N. Farrokhzad-Ershad, B. Rahrovi, M. Ehsani, "Brushless Doubly-Fed Induction Machine With Feed-Forward Torque Compensation Control", *Proceeding of the IEEE/TPEC*, pp. 1-6, Texas, USA, Feb. 2021.

[13] J. Poza, E. Oyarbide, I. Sarasola, and M. Rodriguez, "Vector Control Design and Experimental Evaluation for the Brushless Doubly Fed Machine," *IET Electric Power Applications*, vol. 3, no. 4, pp. 247-256, July 2009.

[14] K. J. Astrom and B. Wittenmark, *Adaptive Control*, 2nd ed. AddisonWesley, 1995, ch. 5.

[15] H. K. Khalil, *Nonlinear Control*, 3rd ed. Prentice Hall, 2002, ch. 8.

[16] H. Mosaddegh-Hesar, X. Liang, M. A. Salahmanesh, M. Ayaz Khoshhava and S. Abdi, "Vector Control of Brushless Doubly-Fed Induction Machines Based on Highly Efficient Nonlinear Controllers," *IEEE Transactions on Industrial Electronics*, doi: 10.1109/TIE.2023.3296811.

[17] H. R. Mosaddegh-Hesar and H. Abootorabi Zarchi, "Maximum Torque per Ampere Control of Brushless Doubly Fed Induction Machine using Variable Structure Approach," *22nd Iranian Conference on Electrical Engineering (ICEE)*, Tehran, Iran, 2014, pp. 677-682.